

High Frequency Welding of Low Carbon Steel Tube

Dr. Paul F. Scott
Thermatool Corp.
East Haven, Connecticut, USA

Introduction:

The prevalent material encountered in pipe and tube fabrication is low carbon steel. It is also the most fascinating because, over the temperature range encountered in forge welding, it behaves as two distinctly different materials. Below about 500 degrees C (932 degrees F), the material exhibits appreciable magnetic permeability (even at high frequency welding frequencies), a relatively low electrical resistivity, and high tensile strength. At temperatures above 800 degrees C (1472 degrees F), the material has the magnetic permeability of free space (air), a relatively high electrical resistance (over five times that at room temperature), and low tensile strength. Several material properties of low carbon steel as a function of temperature are plotted in Figure 1 and 2.

When considering the heating of the weld "Vee" to the forge temperature that occurs in high frequency pipe and tube welding, one is forced to believe that this heating cannot be uniform. At the induction coil or contact end of the "Vee", the material starts heating from room temperature. Because of the high magnetic permeability and low electrical resistivity at temperatures below 500 degrees C, the Electrical Reference Depth, that determines how far the high frequency current penetrates the material, is very small (comparable to that of copper). Heating must occur at the very surface of the "Vee" edges, and because the current is highly concentrated, the temperature must rise very quickly. Further toward the apex of the weld "Vee", beyond the point where the temperature has risen to 800 degrees C, loss of magnetic permeability and increased electrical resistivity cause the Electrical Reference Depth to increase to several millimeters. The high frequency current penetrates much deeper into the "Vee" edges and the high frequency heating is distributed over a much larger volume. Thus as the apex of the "Vee" is approached, the rate of heating is slower and to a greater depth in the "Vee" edges.

Theoretical analysis has been conducted for high frequency "Vee" heating, and it has been previously shown that the high frequency welding process can operate in two distinct modes - the Electric Power mode and the Thermal mode¹. When in the Thermal mode, the heating of the weld "Vee" is controlled primarily by the tube material's Thermal Reference Depth. When in the Electric Power mode, the "Vee" heating process is controlled primarily by the Electrical Reference Depth. The mode in which the process operates is determined by the welding frequency, weld "Vee" length, and the mill speed. Higher welding frequencies, longer "Vee" lengths, and slower mill speeds cause the process to operate in the

¹ Scott, Paul; The Effects of Frequency in High Frequency Welding; Tube 2000 Toronto, ITA Conference, 1996

Thermal mode. Lower welding frequencies, shorter weld “Vee” lengths, and faster mill speeds cause the process to operate in Electric Power mode.

It has also been shown that it is advantageous to operate the process in the Thermal mode. This results in:

- Lower weld power requirements
- Lower impeder flux, hence reducing the likelihood that the impeder magnetically saturates
- Reduced sensitivity to process parameter variation

While this analysis has been able to accurately predict the over-all features of the high frequency welding process for low carbon steel, it has not been possible to use it to predict detailed temperature profiles in the weld “Vee” because the equations require fixed values for the material properties that do not depend on temperature.

To obtain reasonable temperature distributions in the weld “Vee” for the purposes of increased process understanding and improvement, a model that couples the temperature dependent electrical and thermal properties must be employed. Such a model has been constructed and solutions for specific welding problems have been found by using finite element, computer solution techniques. The balance of this paper describes the model and shows results obtained using it.

Description of the Modeling Technique:

Heating of the weld “Vee” for the high frequency pipe and tube welding process is governed by the electric current distribution and thermal conduction. The distribution of the electric current is governed by the Electrical Reference Depth and by the “proximity” effect. Both of these are fully described by Maxwell’s equations for electric and magnetic fields. Thermal conduction can be accurately described by the Biot Fourier equation. Both of these equations can be written in a way that accounts for thermal/spatial variation of the tube material parameters.

Starting with the thermal conduction problem and considering the “vee” geometry shown in Figure 3, the Biot Fourier equation in integral form can be written as:

$$\underbrace{\iint_S K(T(x, y)) \vec{\nabla} T(x, y) \cdot \vec{n} da}_{\text{Heat Flowing Out to Adjacent Elements Due to Thermal Conduction}} + \underbrace{\iiint_V q dv}_{\text{Heat Generated by Electric Current in Volume}} = \underbrace{\iiint_V C(T(x, y)) \rho_o \frac{dT(x, y)}{dt} dv}_{\text{Change in Temperature Due to Change in Heat Content}} \quad (1)$$

where the time derivative has been replaced with the spatial derivative in y to convert the problem from coordinates relative to the tube (LaGrangian) to coordinates relative to the mill (Eulerian):

$$\frac{dT(x,t)}{dt} = \left[\frac{dT(x,y)}{dy} \right] \left[\frac{dy}{dt} \right] = v_o \frac{dT(x,y)}{dy} \quad (2)$$

In the above relationships:

$T(x, y)$ is the relative temperature in the tube material surrounding the “Vee” ($T = 0$ is taken as the starting temperature),

x is the direction normal from the “Vee” edge into the material ($x = 0$ is at the edge of the “Vee”),

y is the direction along the “Vee” edge ($y = 0$ is at the beginning of the “Vee” where the high frequency current starts to flow),

K is the thermal conductivity of the tube material (a function of temperature),

q is the heat per volume generated in the “Vee” material by the high frequency current,

C is the product of the specific heat (C_p) and mass density (ρ) for the tube material (a function of temperature),

and v_o is the mill speed.

To construct the finite element model for the temperature distribution, we evaluate the integrals in Equation 1 over a small, but finite volume of the tube material (see Figure 4). As we are assuming negligible temperature variation over the thickness of the tube material, the elements have dimension Δx by Δy by g , where g is the wall thickness of the tube. The assumption is that each element is small enough that its material properties are essentially constant. The continuous dimensions x and y become the discrete dimensions:

$$x = n \Delta x \quad (3)$$

and

$$y = m \Delta y \quad (4)$$

where n and m are integers.

Thus we derive the discrete relationship:

$$\begin{aligned} & \frac{(K(n-1,m) + K(n,m))}{2} \frac{(T(n-1,m) - T(n,m))}{\Delta x} g \Delta y + \frac{(K(n+1,m) + K(n,m))}{2} \frac{(T(n+1,m) - T(n,m))}{\Delta x} g \Delta y \\ & + q(n,m) \Delta x \Delta y g = C(n,m) v_o \frac{(T(n,m+1) - T(n,m))}{\Delta y} \Delta x \Delta y g \end{aligned} \quad (5)$$

from the continuous relationship in Equation 1. This result is then rearranged to obtain an incremental relationship from which $T(n, m+1)$ can be obtained from $T(n-1, m)$, $T(n, m)$ and $T(n+1, m)$:

$$\begin{aligned} T(n, m+1) = T(n, m) & + \frac{\Delta y}{C(n,m) v_o \Delta x^2} \frac{(K(n-1,m) + K(n,m))}{2} (T(n-1,m) - T(n,m)) \\ & + \frac{\Delta y}{C(n,m) v_o \Delta x^2} \frac{(K(n+1,m) + K(n,m))}{2} (T(n+1,m) - T(n,m)) + \frac{\Delta y}{C(n,m) v_o} q(n,m) \end{aligned} \quad (6)$$

This equation is solved iteratively in the y , or $m\Delta y$ direction, starting from $m = 0$ where:

$$T(n, m = 0) = 0 \text{ for all } n, \quad (7)$$

and in each iteration, the boundary conditions

$$\left. \frac{dT(x,y)}{dx} \right|_{x=0} = 0 \text{ for all } y \quad (8)$$

and

$$T(x \rightarrow \infty, y) = 0 \quad (9)$$

are employed. Equation 8 insures that no heat is lost at the “Vee” edge and Equation 9 insures that far away from the “Vee” edge no heating occurs.

To find the heating in each element due to the electric current, we start by finding the magnetic field, H , in each element. For a given element n, m ; the magnetic field is governed by:

$$\frac{d^2 \vec{H}(n \Delta x + \eta, m \Delta y)}{d\eta^2} - j 2\pi f \mu (T(n,m)) \sigma (T(n,m)) \vec{H}(n \Delta x + \eta, m \Delta y) = 0 \quad (10)$$

where:

$\vec{H}(n \Delta x + \eta, m \Delta y)$ is the magnetic field in element n, m and η is valid in the interval $-\frac{\Delta x}{2} \leq \eta \leq \frac{\Delta x}{2}$,

f is the frequency of the high frequency current (welding frequency),

$\mu(T(n, m))$ is the magnetic permeability of the tube material (a function of temperature),

and $\sigma(T(n, m))$ is the electrical conductivity of the tube material (a function of temperature).

This equation can be shown to have the solution:

$$\vec{H}(n \Delta x + \eta, m \Delta y) = \left[A(n, m) e^{(1+j)\eta/s(T(n, m))} + B(n, m) e^{-(1+j)\eta/s(T(n, m))} \right] \vec{i}_z \quad (11)$$

where the field is assumed oriented in the z direction. The variable s in the above is the Electrical Reference Depth, which is now a function of temperature, and defined by:

$$s(T(n, m)) = \sqrt{\frac{1}{\pi f \mu(T(n, m)) \sigma(T(n, m))}} \quad (12)$$

and A(n, m) and B(n, m) are arbitrary constants chosen to match the boundary conditions.

At the joining edges of elements both the magnetic field and its associated electric field must be continuous. Further, to find the heating of the element due to the high frequency current, we will also need the current density within the element. The electric field and current density are found from:

$$\vec{\nabla} \times \vec{H}(n \Delta x + \eta, m \Delta y) = \vec{J}(n \Delta x + \eta, m \Delta y) \quad (13)$$

and

$$\vec{J}(n \Delta x + \eta, m \Delta y) = \sigma(T(n, m)) \vec{E}(n \Delta x + \eta, m \Delta y) \quad (14)$$

Substituting Equation 11 into Equations 13 and 14, results in:

$$\vec{J}(n \Delta x + \eta, m \Delta y) = \begin{bmatrix} -A(n, m) \frac{(1+j)}{s(T(n, m))} e^{(1+j)\eta/s(T(n, m))} \\ + B(n, m) \frac{(1+j)}{s(T(n, m))} e^{-(1+j)\eta/s(T(n, m))} \end{bmatrix} \vec{i}_y \quad (15)$$

and

$$\vec{E}(n \Delta x + \eta, m \Delta y) = \begin{bmatrix} -A(n, m) \frac{(1+j)}{s(T(n, m)) \sigma(T(n, m))} e^{(1+j)\eta/s(T(n, m))} \\ + B(n, m) \frac{(1+j)}{s(T(n, m)) \sigma(T(n, m))} e^{-(1+j)\eta/s(T(n, m))} \end{bmatrix} \vec{i}_y \quad (16)$$

We now match conditions at the boundary between elements to determine the constants $A(n, m)$ and $B(n, m)$:

$$\begin{aligned} A(n, m) e^{(1+j)\Delta x/2s(T(n, m))} + B(n, m) e^{-(1+j)\Delta x/2s(T(n, m))} \\ = A(n+1, m) e^{-(1+j)\Delta x/2s(T(n, m))} + B(n+1, m) e^{(1+j)\Delta x/2s(T(n, m))} \end{aligned} \quad (17)$$

and

$$\begin{aligned} -A(n, m) \frac{(1+j)}{s(T(n, m)) \sigma(T(n, m))} e^{(1+j)\Delta x/2s(T(n, m))} \\ + B(n, m) \frac{(1+j)}{s(T(n, m)) \sigma(T(n, m))} e^{-(1+j)\Delta x/2s(T(n, m))} \\ = -A(n+1, m) \frac{(1+j)}{s(T(n+1, m)) \sigma(T(n+1, m))} e^{-(1+j)\Delta x/2s(T(n+1, m))} \\ + B(n+1, m) \frac{(1+j)}{s(T(n+1, m)) \sigma(T(n+1, m))} e^{(1+j)\Delta x/2s(T(n+1, m))} \end{aligned} \quad (18)$$

With proper adjustment of the boundary conditions on the end elements, for a problem divided into N elements in the x direction, this results in a system of $2*N$ linear equations with $2*N$ unknowns, so the A 's and B 's are uniquely determined for each value of n at a given iteration of m . At the "Vee" edge ($n = 0$), we require the magnetic field to have a constant real value of H_0 . This constrains the total current flowing along the edge to have zero divergence. At the N^{th} element $A(N, m)$ is set equal to zero to insure the remaining magnetic field decays to zero.

Having determined the A's and B's at each value of m (each iteration of Equation 6), the heating due to the high frequency current is found by putting these values into Equation 15 for J and evaluating:

$$q(n,m) = \frac{1}{\Delta x} \int_{-\Delta x/2}^{\Delta x/2} \frac{1}{\sigma(T(n,m))} |J(n \Delta x + \eta, \Delta y)|^2 dx \quad (19)$$

which is then used to evaluate Equation 6.

The procedure above gives that the temperature distribution in the “Vee” that results from a given “Vee” current, indirectly specified through H_0 . Other quantities such as the current density, the power distribution, and electric and magnetic fields are available as well.

A model based on the concepts outlined above was developed using an analysis program called Matlab and coded in its interpretive language. Plots of the temperatures and fields are available as output from this model. Another useful output is a color map showing the temperature distribution colored regions in a graphical “Vee”. These plots have been assembled into “computer movies” that aid in visualizing how the “vee” heats when it is high frequency welded.

Results from Simulation of Various Pipe and Tube Welding Conditions:

The first example is a 50 mm diameter by 2 mm wall thickness tube welded at 150 meters per minute. Figures 5 and 6 show the temperature distributions from the beginning of the “Vee” to its apex at welding frequencies of 200 kHz and 400 kHz respectively. The tube quickly heats to about 900 degrees C (50% of the forge temperature) in the first 20% of the “vee” length. The change in material properties then causes the “Vee” heating to penetrate more slowly and more deeply into the material, following the change in Electrical Reference Depth. This explains why the most of the “vee” length glows red when low carbon steel is high frequency welded. This is distinctly different from what is observed with austenetic materials.

In this example, the process is operating in the Electric Power Mode. It can be seen that at 200 kHz, the heating is further into the strip edge than at 400 kHz, and more squeeze-out will be required.

Figures 7 and 8 compare the temperature and power distribution at the apex for the two cases above. It can be seen that the power is concentrated in a channel whose depth is determined by the location of the transition temperature. It can also be seen that the temperature distribution follows the shape determined by the high frequency current density distribution in the strip edge. Thus, the process is clearly operating in the Electric Power Mode. Although it is not

obvious from these normalized plots, more power is required when the tube is welded at 200 kHz than when it is welded at 400 kHz.

To further emphasize the effects of the welding modes, we also examined a 150 mm by 8 mm steel tube being welded at 40 meters per minute. Figures 9 and 10 represent the temperature distributions along the “Vee” at 100 kHz and 400 kHz. The family of curves at 400 kHz shows somewhat shallower heating of the “Vee” than the set for 100 kHz. Figures 11 and 12 show the relative power and temperature distributions at the apex at 100 kHz and 400 kHz. In the 100 kHz case, the process is just entering the Thermal Mode. In the 400 kHz case, Thermal Mode has been fully achieved. It can be seen that the temperature distribution is determined by thermal diffusion and little is to be gained by further increasing welding frequency.

Finally we look at the same two tubes for power delivered by the welder as a function of frequency. Note the linear relationship for the smaller tube at the lower welding frequencies shown in Figure 13. This corresponds to Electric Power Mode operation of the process for the for frequencies below 600 kHz. For the larger tube, the square root relationship in Figure 14 corresponds to Thermal Mode operation of the process at all frequencies.

Conclusions:

Finite element modeling can be used to extend our understanding of the high frequency welding process. The welding of low carbon steel, where the material properties undergo violent change as the material heats from room temperature to the forge temperature, is an example of where these techniques are necessary to achieve detailed results.

While heating along the “Vee” is not uniform due to the temperature dependence of the material properties, the distinct difference between the “Thermal Mode” and The “Electric Power Mode” as predicted by the linear theory is still obvious.

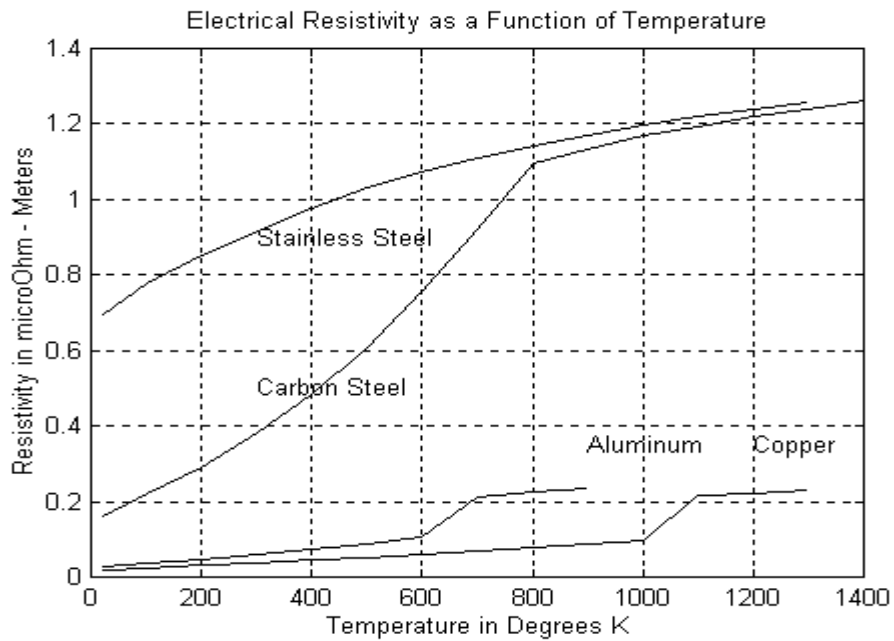


Figure 1 - Temperature Dependence of Material Properties

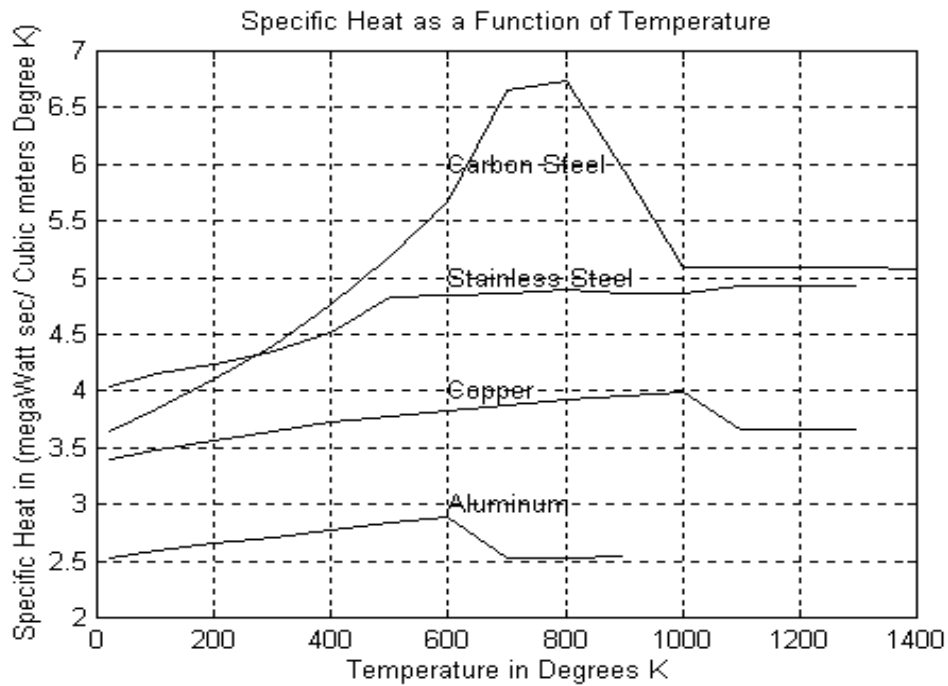


Figure 2 - Temperature Dependence of Material Properties

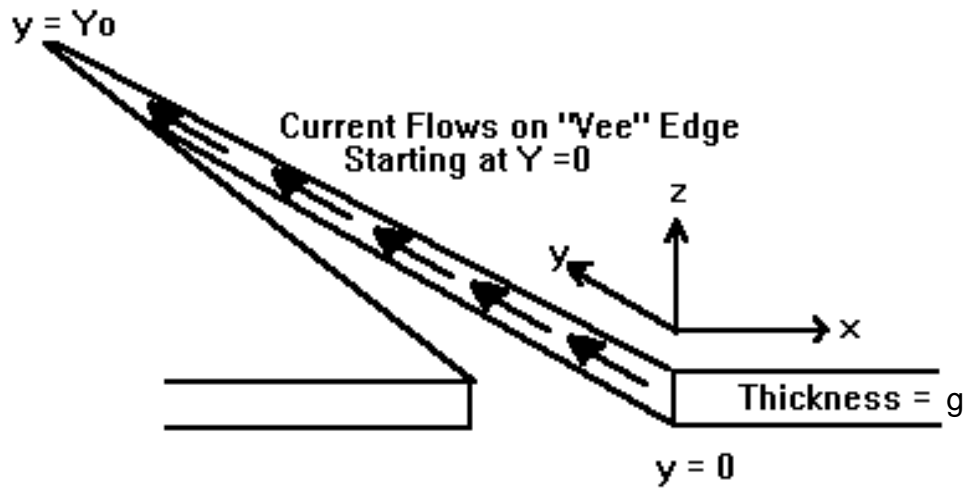


Figure 3 - Geometry of Weld "Vee" Used in Analysis

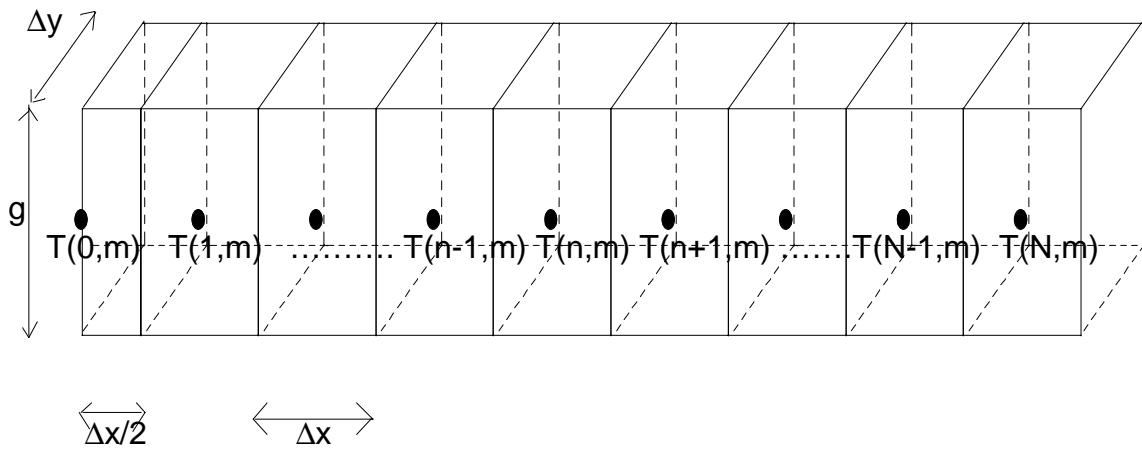


Figure 4 - Geometry of Finite Elements at "Vee" Edge

Steel Tube: 200 kHz, 50 mm OD x 2 mm Wall at 150 M/Min

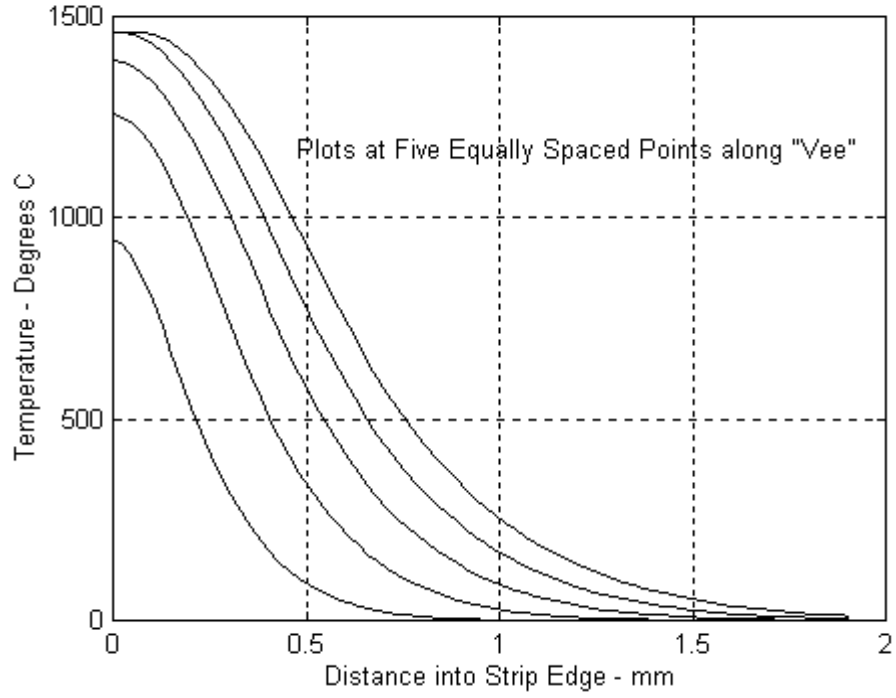


Figure 5

Steel Tube: 400 kHz, 50 mm OD x 2 mm Wall at 150 M/Min

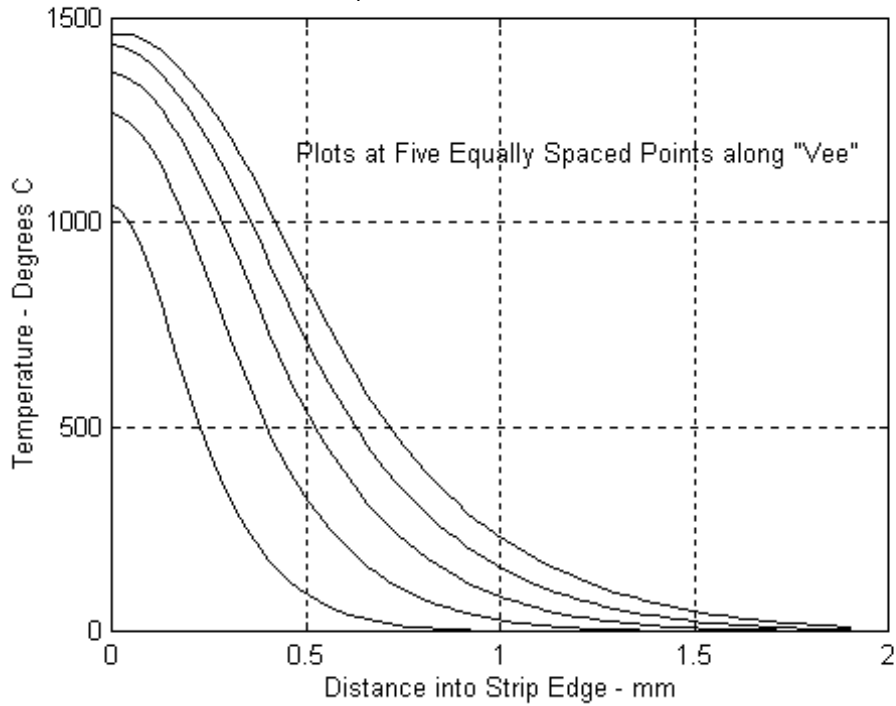


Figure 6

Steel Tube: 200 kHz, 50 mm OD x 2 mm Wall at 150 M/Min

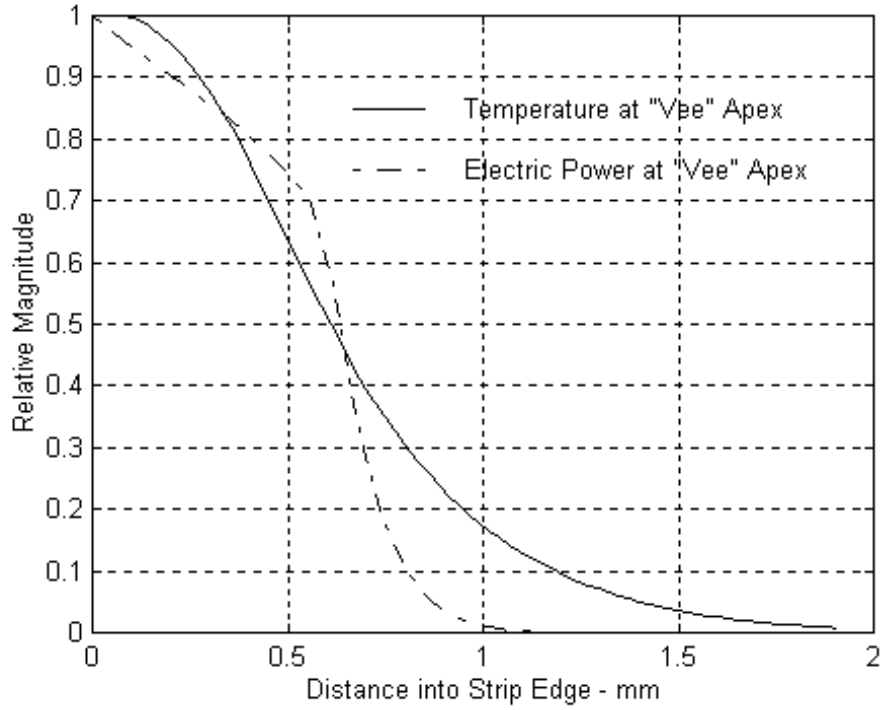


Figure 7

Steel Tube: 400 kHz, 50 mm OD x 2 mm Wall at 150 M/Min

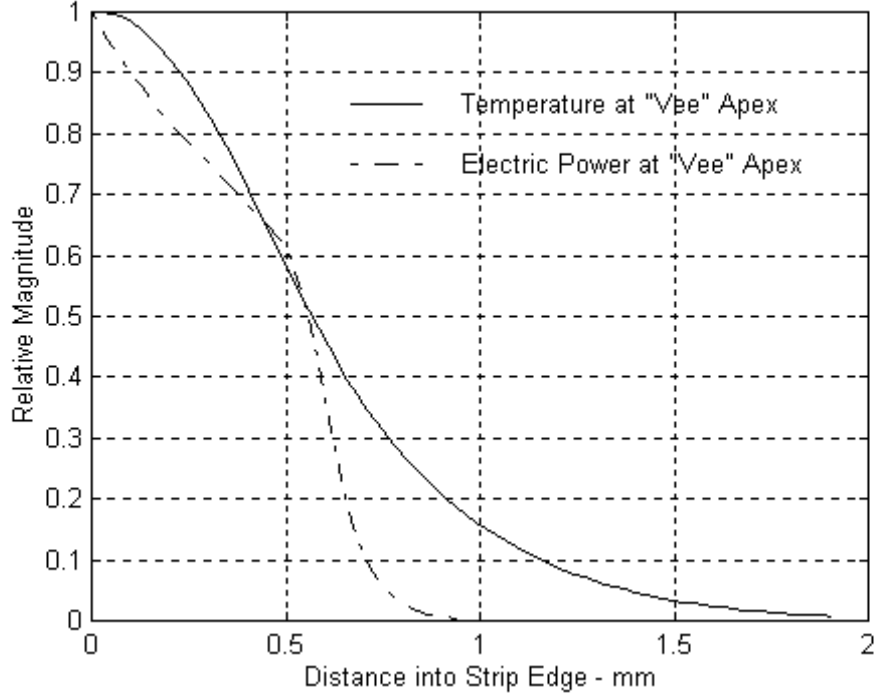


Figure 8

Steel Tube: 100 kHz, 150 mm OD x 8 mm Wall at 40 M/Min

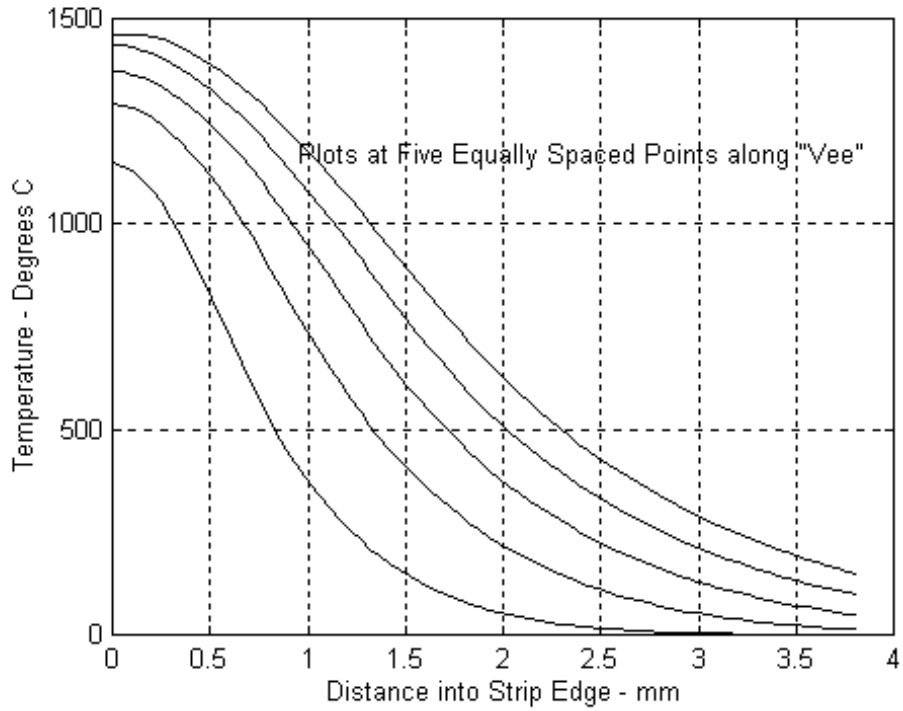


Figure 9

Steel Tube: 400 kHz, 150 mm OD x 8 mm Wall at 40 M/Min

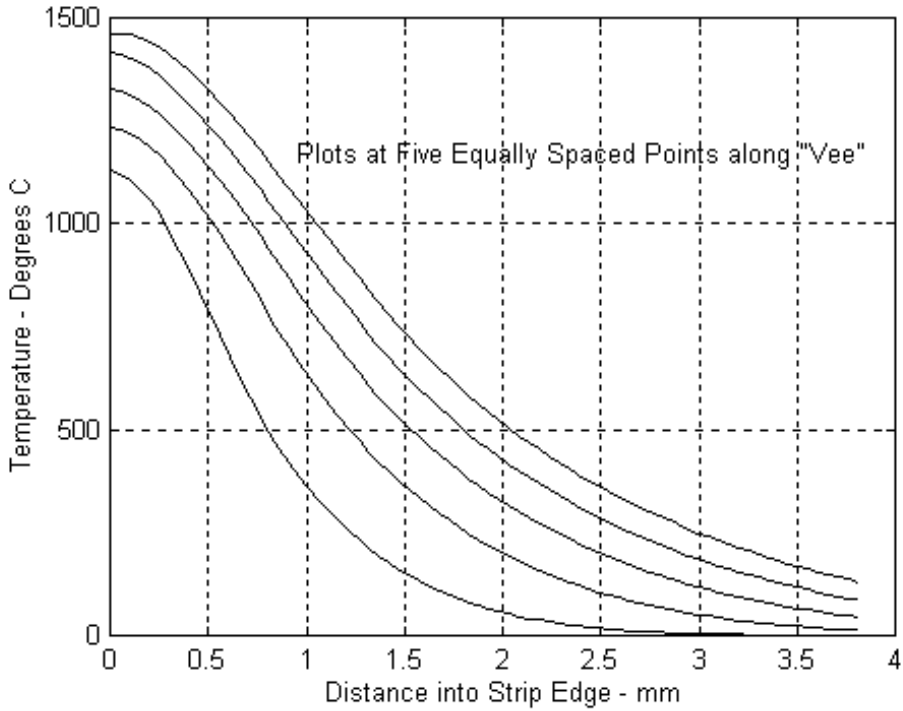


Figure 10

Steel Tube: 100 kHz, 150 mm OD x 8 mm Wall at 40 M/Min

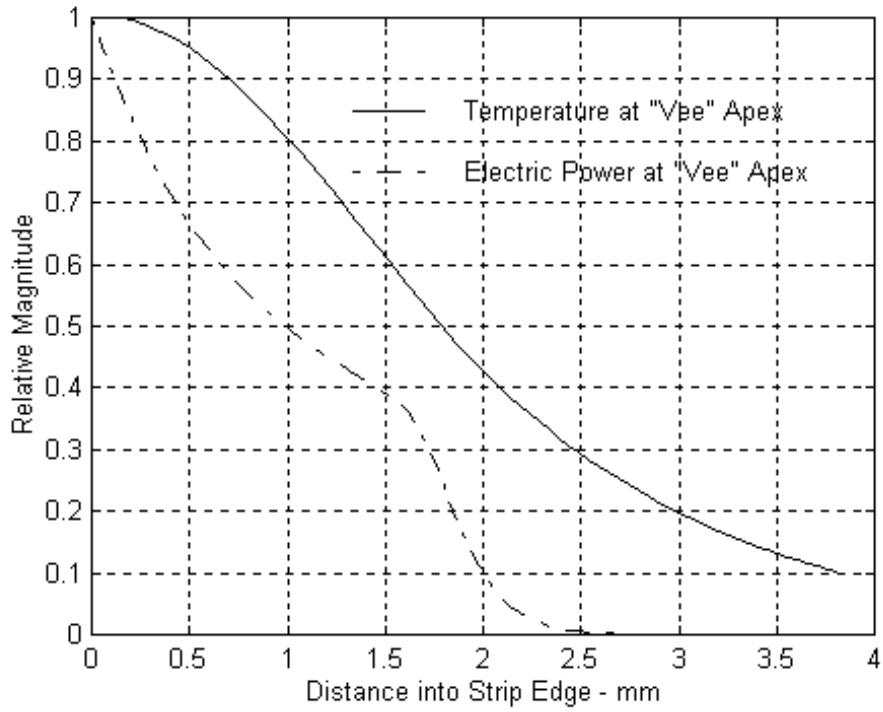


Figure 11

400 kHz, 8 mm Wall, 150 mm "Vee" at 40 M/Min

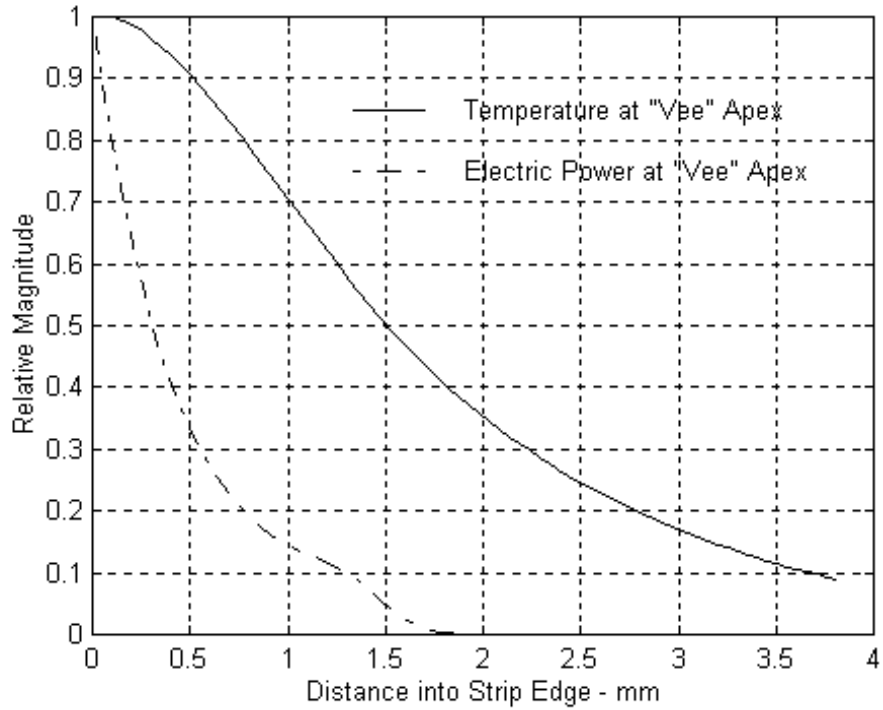


Figure 12

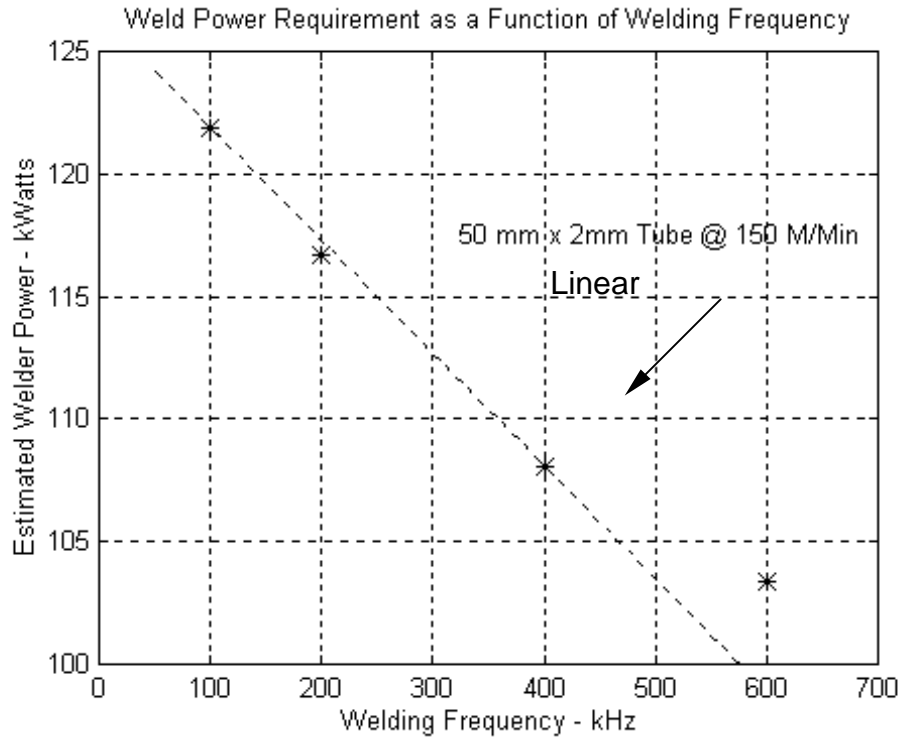


Figure 13

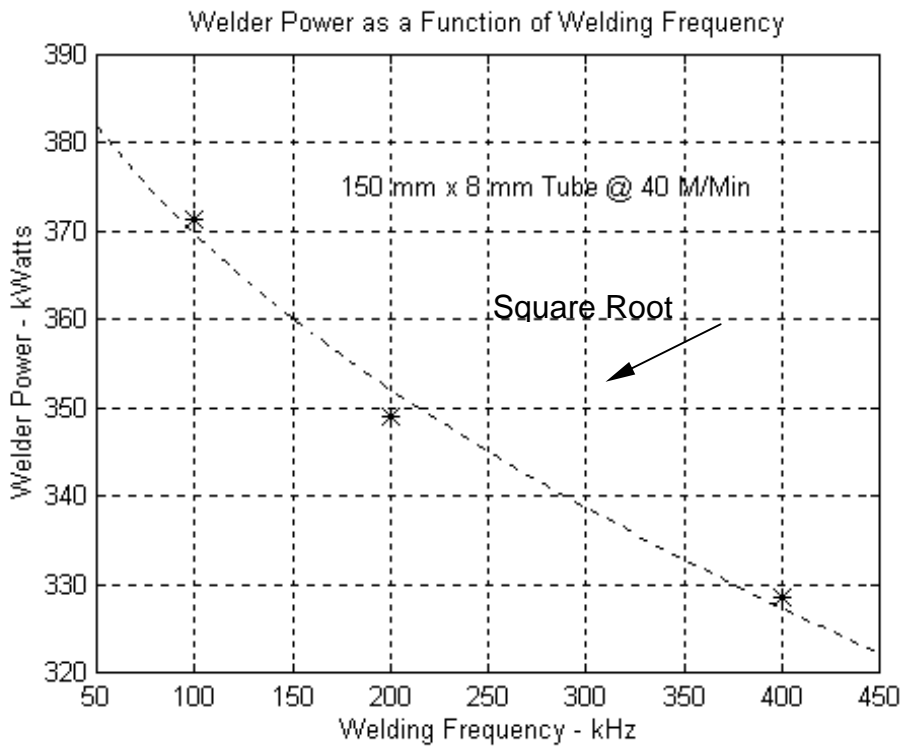


Figure 14